

Intratumoral Treatment of Melanoma Tumors with Large Surface Area Microparticle Paclitaxel and Synergy with Immune Checkpoint Inhibition

Holly A Maulhardt¹, Alyson M Marin¹, Gere S diZerega^{1,2}

¹US Biotest, Inc, San Luis Obispo, CA, USA; ²Nanology, LLC, Fort Worth, TX, USA

Correspondence: Gere S diZerega, US Biotest, Inc, 231 Bonetti Drive, Suite 240, San Luis Obispo, CA, 93401, USA, Tel +01 805 595 1300, Email Gere.diZerega@usbiotest.com

Abstract: The effects of intratumoral (IT) large surface area microparticle paclitaxel (LSAM-PTX) alone and in combination with systemic administration of the programmed cell death protein antibody (anti-mPD-1) were evaluated in a syngeneic murine model of melanoma. Groups of mice with subcutaneously implanted Clone M3 (Cloudman S91) tumors were treated with single and combination therapies. Tumor volume (TV) measurements, body weights, and clinical observations were followed in-life. At end of study, tumor-site tissues were collected, measured, and processed for flow cytometry along with blood and lymph nodes. The combination of LSAM-PTX + anti-mPD-1 resulted in an antitumoral response, which produced a significant decrease in TV compared to control animals. TV decreases also occurred in the LSAM-PTX and anti-mPD-1 groups. Flow cytometry analysis found increases in granulocytes and M2 macrophages and decreases in dendritic cells (DC) and monocytic myeloid-derived suppressor cells (M-MDSC) in tumor-site tissues. Increases in granulocytes and decreases in CD4+ T cells, macrophages, and M1 macrophages were found in the blood of animals administered the combination treatment. Increases in natural killer (NK) cells were found in lymph node tissue in the combination treatment group. These findings suggest that IT LSAM-PTX may provide benefit in the local treatment of melanomas and may synergize with systemic anti-PD-1 therapy, leading to additional tumoricidal outcomes without added systemic toxicity.

Keywords: clone M-3, nanopac, combinatorial immunotherapy, PD-1

Introduction

Combinations of immune checkpoint blockade with chemotherapy, targeted, oncolytic, or anti-angiogenic treatments have shown encouraging results.¹⁻⁴ Transdermal drug delivery systems, such as liposomes, micelles, hydrogels, and emulsions, can facilitate skin permeation and deposition resulting in continuous tumor cell drug exposure.^{3,5,6} The approval of talimogene laherparepvec, an attenuated herpesvirus expressing human granulocyte-macrophage colony-stimulating factor (huGM-CSF), for the intralesional treatment of cutaneous, subcutaneous, and nodal lesions established intratumoral (IT) therapy for melanoma treatment.⁷

Previously, we reported that IT administration of large surface area microparticle docetaxel (LSAM-DTX) reduced primary and metastatic orthotopic breast cancer in a syngeneic mouse model and anti-tumor activity was further enhanced by addition of systemic treatment with the cytotoxic T lymphocyte antigen 4 antibody (anti-mCTLA-4).⁸ This report describes the synergistic reduction in a murine melanoma tumor model (Clone M-3 (Cloudman S91)) following IT administration of a large surface area microparticle paclitaxel (LSAM-PTX) in combination with systemic administration of the programmed cell death protein 1 antibody (anti-mPD-1). LSAM-DTX and LSAM-PTX are investigational products not yet approved for use by the US Food and Drug Administration.

The long residence time of LSAM-PTX within the tumor acts as a drug depot, resulting in continuous release of paclitaxel, exposing tumor cells to high, therapeutic levels of chemotherapeutic for several weeks.⁹ In addition to the tumoricidal effects of local LSAM-PTX and LSAM-DTX therapy, immunomodulation, including increases in the concentration of innate and

adaptive immune cells in the tumor and peripheral blood have also been reported in early-phase clinical studies.^{9–12} Immune modulation has also been found in preclinical investigations including increases in immune effector cells in the peripheral blood following LSAM-DTX injections into mouse models of renal (Renca tumors)¹³ and breast cancer (4T-1 tumors).⁸ In this study, local LSAM-PTX alone and in combination with systemic anti-mPD-1 was evaluated for efficacy and immunomodulation in a syngeneic murine orthotopic melanoma model.

Materials and Methods

Animals

Female DBA/2N mice (DBA/2NCrI, Charles River GmbH, Sulzfeld, Germany) were 5 to 10 weeks old on study Day 0. Animals were fed ad libitum water and V1126-000 Complete Feed (ssniff Spezialdiäten GmbH, Soest, Germany) and housed maximum 4/ventilated cage on a 12-h light cycle at $22 \pm 2^\circ\text{C}/45\text{--}65\%$ humidity. Daily monitoring for clinical signs and abnormalities and three-time weekly weighing occurred for the duration of the study.

Deviations of the health status of the animals were documented, and animals were euthanized individually before study termination when ethical abortion criteria were reached (body weight loss $\geq 20\%$, signs of sickness, ascites, tumor diameter ≥ 1.8 cm, or tumor ulceration).

This animal study was approved by the Ethics Committee for Animal Experimentation and is registered by Freiburg's regional board. Mice were handled according to German animal welfare law and GV-SOLAS guidelines. Health monitoring of the animal facility at Reaction Biology was done according to FELASA guidelines quarterly by examination of sentinel animals.

Tumor Implantation and Treatment

The original melanocyte cell line Clone M-3 [Cloudman S91 melanoma] was acquired from the American Type Cell Collection (ATCC Cat. No. CCL-53.1) and passaged once in vivo, resulting in clone M3(Z1) used in the study. Cells were grown at 37.5°C , 5% CO_2 in RPMI 1640 Glutamax 1 (Gibco by Life Technologies, Paisley, UK), 10% FCS, 1% penicillin/streptomycin and expanded as $70\text{--}90\%$ confluent cultures routinely split using trypsin/EDTA. On study Day 0, 1.0×10^6 cells were suspended in $100 \mu\text{L}$ phosphate buffered saline (PBS) and implanted into the left mammary fat pad.

LSAM-PTX was supplied by Critech, Inc. (Lawrence, KS, USA) as a dry powder reconstituted at time of use as a 24.0 mg/mL suspension in 0.39% polysorbate 80/ 0.9% sodium chloride and administered IT at a $50.0 \mu\text{L}$ fixed injection volume on Days 10, 14, and 18 alone or in combination with IP anti-mPD-1 (Clone RMP1-14; Bio X Cell, Inc., Lebanon, NH, USA) at 10.0 mg/kg . Anti-mPD-1 treatment was initiated 48 hr following IT LSAM-PTX therapy on Days 12, 15, and 18. Additional groups of animals received anti-mPD-1 monotherapy (10 mg/kg on Days 12, 15 and 18) or IT vehicle control + IP isotype control (Rat IgG2a, Bio X Cell, Inc., Lebanon, NH, USA, vehicle-isotype control) at the same dose and schedule as experimental treatments, or were left untreated (Table 1). IT doses were delivered using a 27G needle with an injection volume deposited at one to four sites within the primary tumor.

Table 1 Treatment Groups

n	Group	Treatment	Dose (mg/kg)	Route of Administration	Treatment Days
8	1	Untreated	–	–	–
8	2	Vehicle control ^a + isotype control	– + 10.0	IT ^b + IP ^c	10, 14, 18 + 12 ^d , 15, 18
8	3	LSAM-PTX	60.0	IT	10, 14, 18
8	4	anti-mPD-1	10.0	IP	12 ^d , 15, 18
8	5	LSAM-PTX + anti-mPD-1	60.0 + 10.0	IT + IP	10, 14, 18 + 12 ^d , 15, 18

Notes: ^aVehicle formulation = 0.39% polysorbate 80 in 0.9% sodium chloride; ^bIntratumoral (IT) administration; ^cIntraperitoneal (IP) administration; ^dInitiated 48-hours following IT therapy.

Scanning electron micrographs for micronized paclitaxel drug substance and LSAM-PTX were shown in a previous publication.⁹ The micronized paclitaxel drug substance had a mean particle size of 2.97- μm and an SSA of 7.11- m^2/g and the LSAM-PTX had a mean particle size of 2.51- μm and an SSA of 29.7- m^2/g .

Tumor Assessment

Tumor volume (TV) was calculated using the formula in Eq. (1):

$$\text{TV}(\text{mm}^3) = \frac{(w^2 * l)}{2} \quad (1)$$

Where w = greatest width and l = greatest length, in mm, of a tumor, $l > w$. Primary TV was determined by caliper measurement three times weekly after start of treatment. During necropsy on Day 20, primary tumors were collected, and volumes and wet weights determined.

Flow Cytometry Analysis

On Day 20, blood, lymph nodes (2 axial and 2 inguinal, pooled) and tumor-site tissues (200–300 mg) were collected and processed for flow cytometry. Blood was collected via retro-orbital vein puncture and immediately transferred into K₂E tubes on ice and erythrocytes were removed using Red Blood Cell Lysis Solution (Miltenyi Biotec, Bergisch Gladbach, Germany). Tumor tissue was disrupted using gentleMACS™ C Tubes containing the enzyme mix of the Tumor Dissociation Kit according to the manufacturer's instructions (Miltenyi Biotec, Bergisch Gladbach, Germany). Single cells were prepared from lymph nodes by squeezing pooled node tissue through a cell strainer. Erythrocytes were removed from nodes as previously described.

The single-cell suspensions were counted and dispensed ($\sim 3 \times 10^6$ cells/sample) in 96 well plates. Cells were washed with PBS and stained for living cells for 30 min with Flexible Viability Stain 780 (FVS780, BD Biosciences, Franklin Lakes, NJ, USA). After washing and centrifugation, samples were incubated with 50 μL Fc block (anti-mouse CD16/CD32 1:50) for 15 min in Flow Cytometry Staining (FACS) buffer. Fifty μL of 2X concentrated master antibody mix (CD3, CD4, CD8a, CD45, CD25, CD11b, Ly6C, Ly6G, F4/80, CD11c, MHC class II, CD206, CD335, CD49b, B220) was added and incubated for 30 min in the dark. Intracellular staining was primed by adding 100 μL fixation/permeabilization buffer and incubating for 30 min. Following centrifugation, cell pellets were resuspended in buffer containing the anti-FOXP3 antibody and incubated for 30 min in the dark. Following washing with a permeabilization buffer, cells were resuspended in FACS buffer and stored at 4°C in the dark for up to 5 days prior to flow cytometry analysis on LSR Fortessa (BD Biosciences, Franklin Lakes, NJ, USA).

Phenotypes of immune cells determined by flow cytometry were used to assess cell populations as % of CD45+ cells. Flow phenotypes were defined as follows: CD3+ cells = CD45+/CD11b-/CD3+, CD4+ T cells = CD45+/CD11b-/CD3+/CD4+, CD8+ T cells = CD45+/CD11b-/CD3+/CD8+, Tregs = CD45+/CD3+/CD4+/CD25+/FoxP3+, B cells = CD45+/CD11b-/CD3-/B220+, NK cells = CD45+/CD11b-/CD3-/CD335+/CD49b+, dendritic cells = CD45+/CD11b+/F4-80-/Ly6G-Ly6C-/CD11cFoxP3+/MHCII+, granulocytes = CD45+/CD11b+/F4-80-/Ly6G+Ly6C-, monocytes (monocytic myeloid-derived suppressor cells (M-MDSC)) = CD45+/CD11b+/F4-80-/Ly6G-Ly6C+, macrophages = CD45+/CD11b+/F4-80+, M1 macrophages = CD45+/CD11b+/F4-80+CD206-/MHCII+, M2 macrophages = CD45+/CD11b+/F4-80+CD206-/MHCII-.

Statistical Analysis

For block-randomization, a robust automated random number generation within individual blocks was used (Microsoft® Excel® 2016, Microsoft Corporation, Redmond, WA, USA). Data of the individual groups were analyzed using descriptive data analysis. Statistical analysis of efficacy data was done using the unpaired Student's *t*-test and one-way ANOVA with Dunnett's post-test. Analysis of flow cytometry data was performed by comparing treatment groups to the IT vehicle + isotype control group using Kruskal–Wallis with Dunn's multiple comparison tests. Data analyses were performed using GraphPad Prism 9.4.1 (GraphPad Software, Inc., San Diego, CA, USA).

Results

Tumor Growth

Ten days after tumor implant, animals were block-randomized into five groups ($n=8/\text{group}$) with group mean TV = 56.8 mm^3 (range $42.8\text{--}66.3 \text{ mm}^3$) and treatments were initiated. On Day 20, the IT LSAM-PTX-treated and IP anti-mPD-1-treated groups showed noticeable nonsignificant inhibition of TV compared to the vehicle-isotype control group and TV was further reduced in the group treated with the combination of IT LSAM-PTX + IP anti-mPD-1 (Figure 1a). When TV and tumor weight was measured following necropsy on Day 20, the combined treatment of IT LSAM-PTX and IP anti-mPD-1 resulted in significant ($p < 0.05$) reduction in both TV (Figure 1b) and tumor weight compared to control-treated animals.

Toxicity

One animal died after LSAM-PTX treatment on Day 10 and one animal treated with the vehicle-isotype control was euthanized on Day 19 due to tumor size criteria. Mean animal weights of all study groups either remained stable or slightly increased. In animals treated with LSAM-PTX a slight and transient weight loss was found on Day 16.

Flow Cytometry

Flow cytometry analysis of tumor-site tissues found that treatment with IT LSAM-PTX + IP anti-mPD-1 showed significant increases in populations of granulocytes ($p < 0.001$) and M2 macrophages ($p < 0.05$) compared to the IT vehicle + IP isotype control group. The combination treatment showed significant reductions in M-MDSC ($p < 0.05$) and DC ($p < 0.01$) in the tumor tissues. Similar to the combination treatment, IT LSAM-PTX alone resulted in significant increases in M2 macrophages ($p < 0.05$). IP anti-mPD-1 monotreatment resulted in significant increases in macrophages ($p < 0.05$) and Treg cells ($p < 0.01$) in the tumor when compared to the control treatment (Figure 2a–c).

In the flow cytometry analysis of whole blood, comparison to the control group found that treatment with IT LSAM-PTX + IP anti-mPD-1 resulted in a significant increase in circulating granulocytes ($p < 0.05$) and a significant reduction in CD4+ T cells ($p < 0.05$), macrophages ($p < 0.001$) and M1 macrophages ($p < 0.05$) (Figure 3a). Animals treated with IT LSAM-PTX alone had a significant decrease in circulating macrophages compared to control ($p < 0.01$).

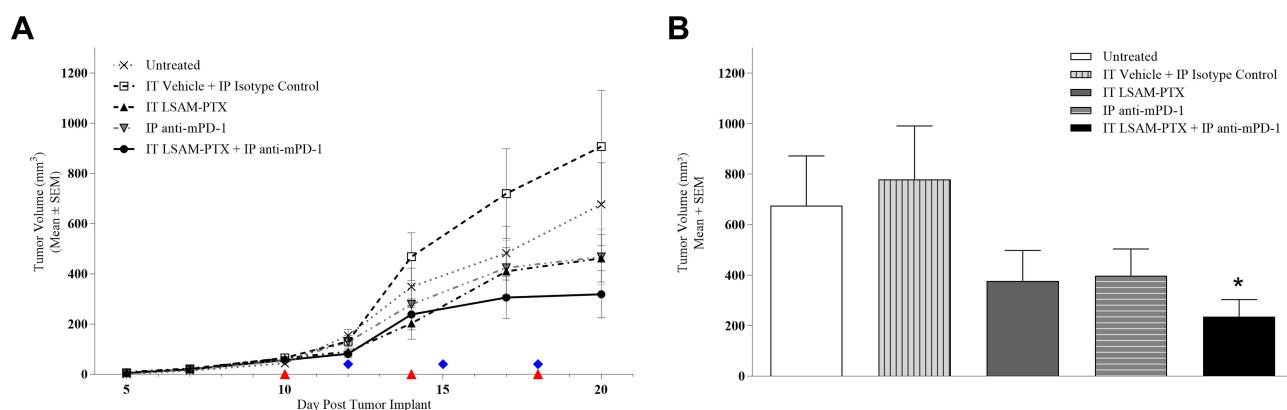


Figure 1 (A) Clone M3 primary tumor volumes. Tumors were implanted on Day 0 and ten days later when mean TV = 56.8 mm^3 animals were randomized to five groups. IT LSAM-PTX ($\sim 60 \text{ mg/kg}$) was administered on Days 10, 14 and 18; IP anti-mPD-1 (10 mg/kg) was administered on Days 12, 15 and 18. Combination IT LSAM-PTX + IP anti-mPD-1 was administered at the same dose and schedules as the single treatments. IT vehicle + IP isotype control treatments were administered on the same schedule as the combination treatments. Untreated animals exhibited tumor growth consistent with previous studies. There were $n=8$ animals/group throughout study with exception of the IT LSAM-PTX group with $n=7$ animals starting at Day 10 and the IT vehicle + IP isotype control group with $n=7$ animals starting at Day 19; no other animals exited prior to Day 20. Data are group mean tumor volumes \pm SEM. Treatment days are indicated as red triangles (LSAM-PTX) or blue diamonds (anti-mPD-1). **(B)** Clone M3 mean tumor volume (mm^3) measured on Day 20 were significantly reduced in animals administered combination IT LSAM-PTX + IP anti-mPD-1 treatment compared to IT vehicle + IP isotype control animals. There were no other statistically significant differences between groups. Data are group mean tumor volumes \pm SEM; * = $p < 0.05$.

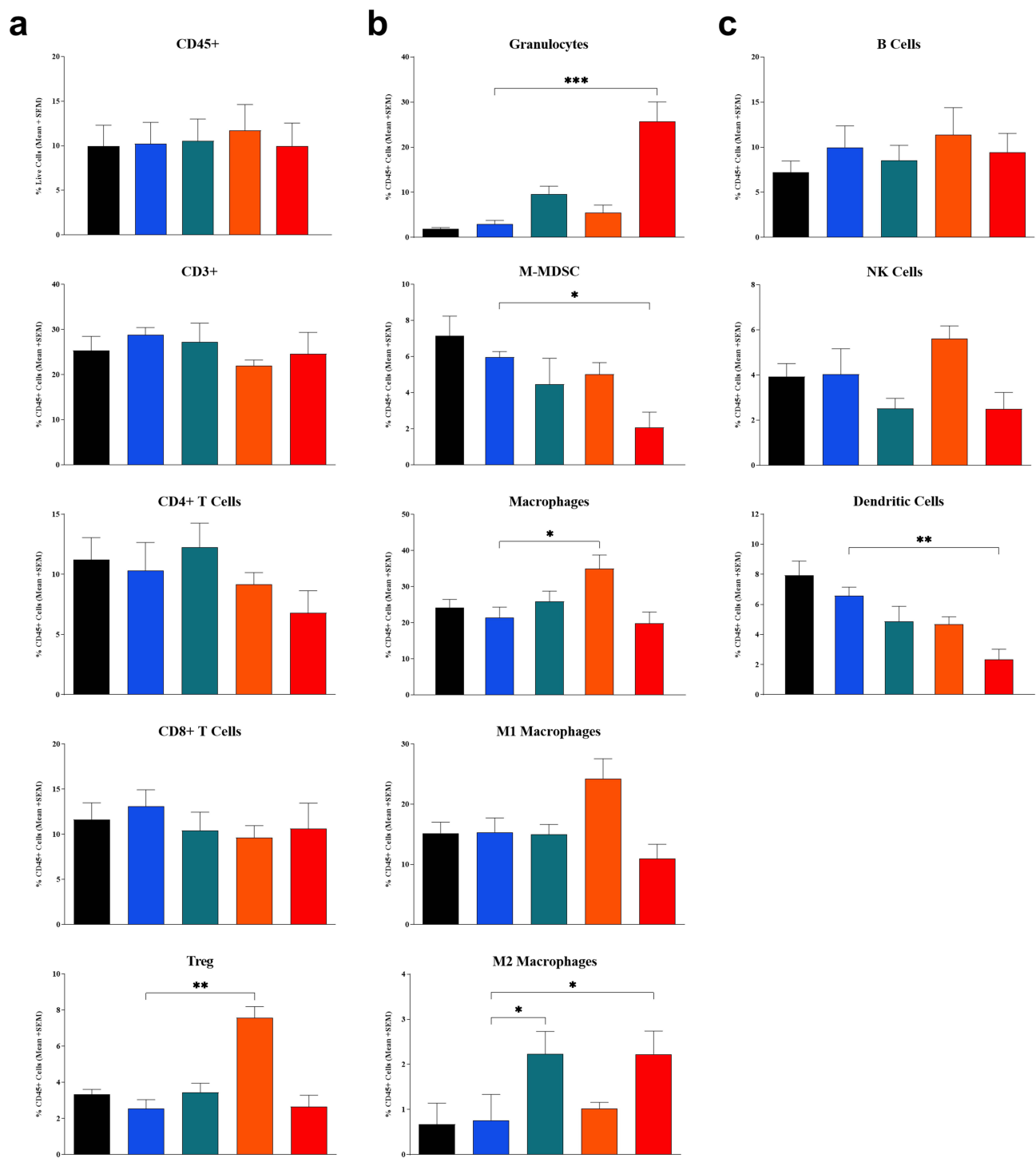


Figure 2 Flow cytometry profile of immune cell population in Clone M3 tumors. Tumors were collected on Day 20 in animals left untreated (black bar) or administered 3 cycles of IT vehicle + IP isotype control (blue bar), IT LSAM-PTX (~60 mg/kg; green bar), IP anti-mPD-1 (10 mg/kg; Orange bar) or IT LSAM-PTX (~60 mg/kg) + IP anti-mPD-1 (10 mg/kg) combination treatment (red bar). (a) CD45+, CD3+, CD4+ T cells, CD8+ T cells, and Treg cells. (b) Granulocytes, M-MDSC, macrophages, M1 macrophages, and M2 macrophages. (c) B cells, NK cells, and dendritic cells. For each population, data are displayed as group mean of %CD45+ cells + SEM. Comparison to IT Vehicle + IP isotype control performed using Kruskal–Wallis and Dunn’s multiple comparisons tests; * = $p < 0.05$; ** = $p < 0.01$; *** = $p < 0.001$.

Interestingly, the only significant difference in immune cell populations in the lymph nodes following treatment with the combination of IT LSAM-PTX + IP anti-mPD-1 control was an increase in NK cells ($p < 0.05$) (Figure 3b). Treatment with anti-mPD-1 alone reduced both M1 and M2 macrophage ($p < 0.05$) populations in the lymph nodes when compared to the IT vehicle + IP isotype control.

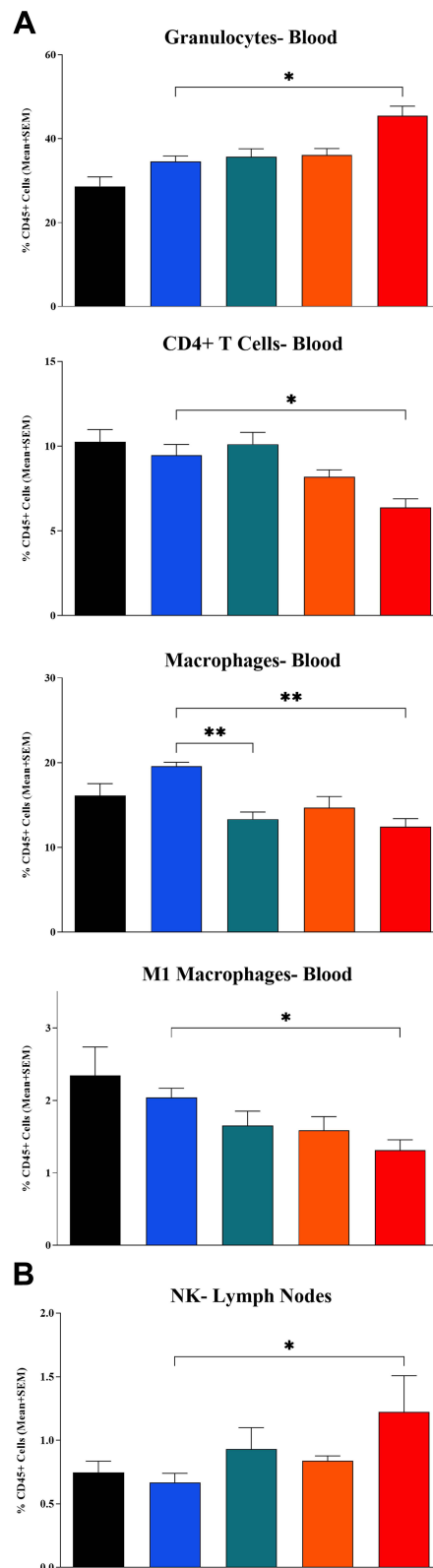


Figure 3 Changes in immune cell populations in mice implanted with Clone M3 tumors. **(A)** Whole blood collected at end of study found changes in granulocytes, CD4+ T cells, macrophages and M1 macrophages. **(B)** Axial and inguinal lymph nodes collected at end of study found significant increases in NK cells. Samples were collected on Day 20 in animals left untreated (black bar) or administered 3 cycles of IT vehicle + IP isotype control (blue bar), IT LSAM-PTX (~60 mg/kg; green bar), IP anti-mPD-I (10 mg/kg; Orange bar) or IT LSAM-PTX (~60 mg/kg) + IP anti-mPD-I (10 mg/kg) combination treatment (red bar). For each population, data are displayed as group mean of %CD45+ cells + SEM. Comparison to IT Vehicle + IP isotype control performed using Kruskal–Wallis and Dunn’s multiple comparisons tests; * = $p < 0.05$; ** = $p < 0.01$.

Discussion

Engineering of large surface area microparticle taxanes (LSAM-PTX and LSAM-DTX) with advances in clinical IT delivery systems have allowed for localized treatment of solid tumors without additional dose-limiting toxicity.^{9,11,14} Ongoing development of other chemotherapies and targeted therapies for IT delivery alone and in combination with currently available treatments including checkpoint inhibitors, radiation, and ablation may make important contributions to patient care.^{15–19} It is possible that LSAM-PTX administration may complement treatment of metastatic disease with traditional therapies such as IV chemotherapy, targeted therapy, immunotherapy, and radiation without adding to systemic toxicities.

Paclitaxel affects many aspects of immune function, including lymphocyte recruitment and activation as well as production of cytokines, IL-12, IFN γ , and TNF α .^{20–24} Paclitaxel given IV enhances immune responses including increased concentrations of tumor-infiltrating lymphocytes that successfully eradicate malignant cells.^{25–27} Paclitaxel may be a particularly strong immunostimulant, as it is able to both activate CD8+ T cells and reduce immunosuppressive cells, such as regulatory T cells^{21–23,28–30} and myeloid-derived suppressor cells (MDSC).^{23,31,32} To maximize tumoricidal effects, it has been suggested that the immune system can be primed with chemotherapy ahead of immunotherapy to re-instate or enhance immunosurveillance.^{24,25,33–36}

Infiltration of adaptive and innate immune cells as well as increases in checkpoint expression by immune cells were found following LSAM-PTX and LSAM-DTX treatment of patients with unresectable locally advanced pancreatic cancer and high-risk non-muscle invasive bladder cancer, respectively.^{10,12} Clinical trials of LSAM-PTX reporting safety and preliminary signals of efficacy have been completed in peritoneal cancer,^{37,38} prostate cancer,⁹ and mucinous cystic pancreatic neoplasms.³⁹ A clinical trial of IT LSAM-PTX treatment of lung cancer (NCT04314895) is ongoing.

Current study shows that IT LSAM-PT further significantly increased tumor cell death when combined with systemic immune checkpoint blockade. Changes in immune cell populations, including increases in local and peripheral granulocytes and reductions in M-MDSC in tumor tissues as well as increases in NK cells in lymph nodes, suggest that the combination of IT LSAM-PTX with anti-mPD-1 may impart anti-tumor immunomodulation.

Continuous cell death resulting from the LSAM-PTX intratumoral depot could affect the immune system by (1) increasing the opportunity for tumor-associated antigens to be released and recognized by the immune system, (2) decreasing the number of cells able to send an immunosuppressive signal, and (3) attracting immune and phagocytic cells to remove tumor cell debris. The observations reported here suggest that prolonged and continuous exposure to tumoricidal levels of paclitaxel in the Clone M3 melanoma model may result in direct tumor killing by the paclitaxel-induced disruption of mitosis followed by tumor cell disruption, making neoantigens available and causing antigen spread within the TME. While a combination of systemic chemotherapy and immunotherapy has the potential to increase efficacy,³³ these regimens are also frequently additive to systemic toxicity. Local administration of LSAM-PTX has the potential to synergize with immunotherapy without added toxic exposure to nontarget organs. The ability to combine “immunocompatible” cytotoxic drugs with checkpoint antibodies increases the direct killing of cancer cells but may also minimize the activation of immunosuppressive and cancer cell pro-survival program responses of systemic chemotherapies.^{2,40}

Previously, in a 4T1-Luc orthotopic breast cancer model, the combination of IT LSAM-DTX + IP anti-CTLA-4 resulted in a significant decrease in TV and thoracic metastasis that was accompanied by increased T cells, NK and NKT cell levels in the tumor and peripheral blood.⁸ In a bilateral syngeneic renal carcinoma tumor model, abscopal-like effects were observed in the reduction of growth in an untreated secondary tumor in which the primary tumor was previously treated with IT LSAM-DTX.¹³ These data are consistent with the hypothesis that the necroptotic response of tumor cells following local LSAM-PTX or LSAM-DTX may stimulate an influx of immune effector cells into the TME, which synergizes with checkpoint inhibitors^{9,13} via both innate and adaptive immunomodulation.

Conclusion

This study found that the combination of local LSAM-PTX and systemic immunotherapy resulted in a significant antitumoral response in the Clone M3 melanoma model and was associated with innate and adaptive anti-tumor immunomodulation. Administration of either IT LSAM-PTX or IP anti-mPD-1 monotherapy resulted in reduction of TV, but to a lesser extent than the combination treatment. No significant toxicity was seen in the combinatorial regimen as shown by animal weight gain as well as lack of adverse clinical events. These findings taken together with favorable immune cell infiltration⁹ and increases in

checkpoint expression following IT LSAM-PTX found in human trials¹² provide support for clinical evaluation of IT LSAM-PTX in combination with immune checkpoint inhibitors for the treatment of melanoma.

Acknowledgments

NanoPac[®] and NanoDoce[®] are registered trademarks of NanOlogy, LLC. The authors would like to thank CritiTech, Inc. for investigational product supply; NanOlogy, LLC. for study funding; and Yazmin Yang for assistance in document preparation.

Disclosure

Holly Maulhardt and Alyson Marin report being full-time employees of US Biotest Inc; Holly Maulhardt and Gere diZerega have a patent 18/154,419 pending to CritiTech Particle Engineering Solutions, LLC; Gere diZerega reports holding a consultant/advisory role, having stock ownership or receiving funding from NanOlogy, LLC.

References

- Kasakovski D, Skrygan M, Gambichler T, Susok L. Advances in targeting cutaneous melanoma. *Cancers*. 2021;13(9):2090. doi:10.3390/cancers13092090
- Bailly C, Thuru X, Quesnel B. Combined cytotoxic chemotherapy and immunotherapy of cancer: modern times. *NAR Cancer*. 2020;2(1):zcaa002. doi:10.1093/narcan/zcaa002
- Xu H, Wen Y, Chen S, Zhu L, Feng R, Song Z. Paclitaxel skin delivery by micelles-embedded carbopol 940 hydrogel for local therapy of melanoma. *Int J Pharm*. 2020;587:119626. doi:10.1016/j.ijpharm.2020.119626
- Kim TK, Vandsemb EN, Herbst RS, Chen L. Adaptive immune resistance at the tumour site: mechanisms and therapeutic opportunities. *Nat Rev Drug Discov*. 2022;21(7):529–540. doi:10.1038/s41573-022-00493-5
- Rigon RB, Oyafuso MH, Fujimura AT, et al. Nanotechnology-based drug delivery systems for melanoma antitumoral therapy: a review. *Biomed Res Int*. 2015;2015:841817. doi:10.1155/2015/841817
- Lacouture ME, Goldfarb SB, Markova A, et al. Phase 1/2 study of topical submicron particle paclitaxel for cutaneous metastases of breast cancer. *Breast Cancer Res Treat*. 2022;194(1):57–64. doi:10.1007/s10549-022-06584-6
- Andtbacka RH, Kaufman HL, Collichio F, et al. Talimogene laherparepvec improves durable response rate in patients with advanced melanoma. *J Clin Oncol*. 2015;33(25):2780–2788. doi:10.1200/JCO.2014.58.3377
- Sharma N, Schmidt CM, Jain S, et al. S2 Improved Resection Rates in Locally Advanced Pancreatic Cancer (LAPC) Following EUS-FNI of Large Surface Area Microparticle Paclitaxel (LSAM Pac). *Am J Gastroenterol*. 2021;116:S1–S2.
- Verco S, Maulhardt H, Baltezar M, et al. Local administration of submicron particle paclitaxel to solid carcinomas induces direct cytotoxicity and immune-mediated tumoricidal effects without local or systemic toxicity: preclinical and clinical studies. *Drug Deliv Transl Res*. 2021;11(5):1806–1817. doi:10.1007/s13346-020-00868-4
- Kates M, Mansour A, Lamm DL, et al. Phase 1/2 trial results of a large surface area microparticle docetaxel for the treatment of high-risk non-muscle invasive bladder cancer. *J Urol*. 2022;208(4):821–829. doi:10.1097/JU.0000000000002778
- Maulhardt H, Verco S, Baltezar M, Marin A, diZerega G. Local administration of large surface area microparticle docetaxel to solid carcinomas induces direct cytotoxicity and immune-mediated tumoricidal effects: preclinical and clinical studies. *Drug Deliv Transl Res*. 2022;2023:1.
- Sharma NR, Lo SK, Hendifar A, et al. Response of locally advanced pancreatic cancer to intratumoral injection of large surface area microparticle paclitaxel: initial report of safety and clinical outcome. *Pancreas*. 2023;52(3):e179–e187. doi:10.1097/MPA.0000000000002236
- Maulhardt HA, Marin AM, diZerega GS. Intratumoral submicron particle docetaxel inhibits syngeneic renal cancer growth and increases CD4+, CD8+, and treg levels in peripheral blood. *Invest New Drugs*. 2020;38(5):1618–1626. doi:10.1007/s10637-020-00922-5
- Verco S, Maulhardt H, Marin A, Verco A. Safety of locally administered large surface area microparticle paclitaxel and docetaxel in combination with standard of care cancer therapies. *J Clin Oncol in Press*. 2023;41(16_suppl):e15187–e15187. doi:10.1200/JCO.2023.41.16_suppl.e15187
- Melero I, Castanon E, Alvarez M, Champiat S, Marabelle A. Intratumoural administration and tumour tissue targeting of cancer immunotherapies. *Nat Rev Clin Oncol*. 2021;18(9):558–576. doi:10.1038/s41571-021-00507-y
- Marabelle A, Tselikas L, de Baere T, Houot R. Intratumoral immunotherapy: using the tumor as the remedy. *Ann Oncol*. 2017; 28(suppl_12):xii33–xii43.
- Moe A, Liow E, Redfern A, et al. A Phase I open label dose-escalation study to evaluate the tolerability, safety and immunological efficacy of sub-urothelial durvalumab injection in adults with muscle-invasive or high-risk non-muscle-invasive bladder cancer (SUBDUE-1, SUB-urothelial DURvalumab injection-1 study): clinical trial protocol. *BJU Int*. 2021;128 Suppl 1:9–17. doi:10.1111/bju.15365
- Rouanne M, Bajorin DF, Hannan R, et al. Rationale and outcomes for neoadjuvant immunotherapy in urothelial carcinoma of the bladder. *Eur Urol Oncol*. 2020;3(6):728–738. doi:10.1016/j.euo.2020.06.009
- Schulz GB, Black PC. Combination therapies involving checkpoint-inhibitors for treatment of urothelial carcinoma: a narrative review. *Transl Androl Urol*. 2021;10(10):4014–4021. doi:10.21037/tau-20-1177
- Chan OT, Yang LX. The immunological effects of taxanes. *Cancer Immunol Immunother*. 2000;49(4–5):181–185. doi:10.1007/s002620000122
- Soliman HH. nab-Paclitaxel as a potential partner with checkpoint inhibitors in solid tumors. *Onco Targets Ther*. 2017;10:101–112. doi:10.2147/OTT.S122974
- Javeed A, Ashraf M, Riaz A, Ghafoor A, Afzal S, Mukhtar MM. Paclitaxel and immune system. *Eur J Pharm Sci*. 2009;38(4):283–290. doi:10.1016/j.ejps.2009.08.009
- Zheng H, Zeltsman M, Zauderer MG, Eguchi T, Vaghjiani RG, Adusumilli PS. Chemotherapy-induced immunomodulation in non-small-cell lung cancer: a rationale for combination chemoimmunotherapy. *Immunotherapy*. 2017;9(11):913–927. doi:10.2217/imt-2017-0052

24. Conway EM, Pikor LA, Kung SH, et al. Macrophages, inflammation, and lung cancer. *Am J Respir Crit Care Med.* 2016;193(2):116–130. doi:10.1164/rccm.201508-1545CI
25. Demaria S, Volm MD, Shapiro RL, et al. Development of tumor-infiltrating lymphocytes in breast cancer after neoadjuvant paclitaxel chemotherapy. *Clin Cancer Res.* 2001;7(10):3025–3030.
26. Moschetta M, Pretto F, Berndt A, et al. Paclitaxel enhances therapeutic efficacy of the F8-IL2 immunocytokine to EDA-fibronectin-positive metastatic human melanoma xenografts. *Cancer Res.* 2012;72(7):1814–1824. doi:10.1158/0008-5472.CAN-11-1919
27. Pasche N, Wulhfard S, Pretto F, Carugati E, Neri D. The antibody-based delivery of interleukin-12 to the tumor neovasculature eradicates murine models of cancer in combination with paclitaxel. *Clin Cancer Res.* 2012;18(15):4092–4103. doi:10.1158/1078-0432.CCR-12-0282
28. Vicari AP, Luu R, Zhang N, et al. Paclitaxel reduces regulatory T cell numbers and inhibitory function and enhances the anti-tumor effects of the TLR9 agonist PF-3512676 in the mouse. *Cancer Immunol Immunother.* 2009;58(4):615–628. doi:10.1007/s00262-008-0586-2
29. Chen DS, Mellman I. Oncology meets immunology: the cancer-immunity cycle. *Immunity.* 2013;39(1):1–10. doi:10.1016/j.immuni.2013.07.012
30. Chen G, Emens LA. Chemoimmunotherapy: reengineering tumor immunity. *Cancer Immunol Immunother.* 2013;62(2):203–216. doi:10.1007/s00262-012-1388-0
31. Chen D, Yu J, Zhang L. Necroptosis: an alternative cell death program defending against cancer. *Biochim Biophys Acta.* 2016;1865(2):228–236. doi:10.1016/j.bbcan.2016.03.003
32. Galluzzi L, Senovilla L, Zitvogel L, Kroemer G. The secret ally: immunostimulation by anticancer drugs. *Nat Rev Drug Discov.* 2012;11(3):215–233. doi:10.1038/nrd3626
33. Champiat S, Tselikas L, Farhane S, et al. Intratumoral immunotherapy: from trial design to clinical practice. *Clin Cancer Res.* 2021;27(3):665–679. doi:10.1158/1078-0432.CCR-20-0473
34. Waitz R, Solomon SB, Petre EN, et al. Potent induction of tumor immunity by combining tumor cryoablation with anti-CTLA-4 therapy. *Cancer Res.* 2012;72(2):430–439. doi:10.1158/0008-5472.CAN-11-1782
35. Rodriguez-Ruiz ME, Vanpouille-Box C, Melero I, Formenti SC, Demaria S. Immunological mechanisms responsible for radiation-induced abscopal effect. *Trends Immunol.* 2018;39(8):644–655. doi:10.1016/j.it.2018.06.001
36. Liu Y, Dong Y, Kong L, Shi F, Zhu H, Yu J. Abscopal effect of radiotherapy combined with immune checkpoint inhibitors. *J Hematol Oncol.* 2018;11(1):104. doi:10.1186/s13045-018-0647-8
37. Williamson SK, Johnson GA, Maulhardt HA, et al. A phase I study of intraperitoneal nanoparticulate paclitaxel (Nanotax(R)) in patients with peritoneal malignancies. *Cancer Chemother Pharm.* 2015;75(5):1075–1087. doi:10.1007/s00280-015-2737-4
38. Mullany S, Miller D, Robison K, et al. Phase II study of intraperitoneal submicron particle paclitaxel (SPP) plus IV carboplatin and paclitaxel in patients with epithelial ovarian cancer surgery. *Gynecol Oncol Rep.* 2020;34(100627):100627. doi:10.1016/j.gore.2020.100627
39. Othman M, Patel K, Krishna S, et al. Early Phase Trial of Intracystic Injection of Large Surface Area Microparticle Paclitaxel for the Treatment of Mucinous Pancreatic Cysts. *Endosc Int Open.* 2022; 10(12):1.
40. Wilson MA, Schuchter LM. Chemotherapy for melanoma. *Cancer Treat Res.* 2016;167:209–229.